

DETC2014-34953

**DESIGN OF A LOW ENERGY, SELF CONTAINED SUBSEA BURROWING ROBOT
BASED ON LOCALIZED FLUIDIZATION EXHIBITED BY ATLANTIC RAZOR CLAMS****Daniel S. Dorsch**Dept. of Mechanical Engineering
Massachusetts Institute of Technology
Cambridge, Massachusetts 02139
Email: dorsch@mit.edu**Amos G. Winter V.**Dept. of Mechanical Engineering
Massachusetts Institute of Technology
Cambridge, Massachusetts 02139
Email: awinter@mit.edu**ABSTRACT**

The Atlantic razor clam (*Ensis directus*) burrows by contracting its valves, fluidizing the surrounding soil and reducing burrowing drag. Moving through a fluidized, rather than static, soil requires energy that scales linearly with depth, rather than depth squared. In addition to providing an advantage for the animal, localized fluidization may provide significant value to engineering applications such as vehicle anchoring and underwater pipe installation. This paper presents the design of a self-actuated, radially expanding burrowing mechanism that utilizes *E. directus*' burrowing methods. The device is sized to be a platform for an anchoring system for autonomous underwater vehicles. Scaling relationships presented allow for design of burrowing systems of different sizes for a variety of applications. The minimum contraction time for a given device size governs how quickly the device must move. Contraction displacement necessary to achieve fluidization is presented. The maximum force for a given size mechanism is also calculated, and allows for sizing actuators for different systems. This paper presents the design of a system that will allow testing of these parameters in a laboratory setting. These relationships provide the optimal sizing and power needs for various size subsea borrowing systems.

INTRODUCTION

There are many applications in which attaching to the seafloor is beneficial. Many animals have found methods to move through soil. While some animals, such as crabs, create burrows, others use methods that allow them to move more efficiently through the soil, such as propagating cracks [1] or wiggling like a snake [2].

There are many different systems that can benefit from improved borrowing and anchoring technologies. Anchoring

autonomous underwater vehicles (AUVs) is one example. Improved anchors could also be used for anchoring larger equipment, such as ships, oil recovery equipment, or repositionable buoys. Lower energy, more efficient systems could reduce the weight needed for an anchor and increase the number of devices that could efficiently use an anchor. For example, current medium sized AUVs do not carry a conventional anchor, as it would be too heavy to use and difficult to retrieve once deployed [3]. A system that is lightweight and could easily detach from the seafloor when desired would be beneficial.

The Atlantic razor clam, *Ensis directus*, exhibits a unique method for burrowing into the soil. This animal is small, about 8 inches long and 1.25 inches wide [4]. It consists of two shell halves that move about a hinge on one side. The shell is spring loaded to open, and muscles cause the shell to close. *E. directus* is fairly weak; Its foot can produce about 10 N of pulling force which should only be enough to pull the animal into packed soil 1-2 cm. In reality, razor clams inhabit soil up to 70 cm deep [5]. They reach this depth by fluidizing the soil around them to reduce drag. It is this ability that makes *E. directus* of interest for a low energy anchoring system.

An *E. directus* based anchor would be much more efficient than current anchoring technologies. The anchoring force it can achieve per energy required to insert it is greater by more than an order of magnitude over currently used systems [6]. Lower energy use is beneficial to any system, but is especially advantageous for energy-limited systems such as AUVs, which run on batteries and have limited capacity.

When burrowing, *E. directus* first pushes its body upward and then quickly contracts its shell. This rapid contraction creates a region of fluidized soil around the animal's shell. This zone is created by fluid being drawn into the region around the animal. An increased fluid to particle ratio (void fraction)

creates a local fluidized zone. Since the area around the clam behaves more like a liquid with particles than a particulate solid, moving downward through this region is just like moving through any other Newtonian fluid. This means there is a constant drag force with depth, where a blunt object moving through soil encounters linearly increasing force with depth [7].

RoboClam is a robot that was developed to test this method of burrowing and discover the ideal performance parameters. It consists of an end effector that moves like and is sized similarly to a razor clam. One pneumatic piston drives the end effector up and down, and a second piston causes the end effector to expand and contract. The end effector is 3 inches long, and 0.6 inches in cross section, expanding 0.25 inches when it is in the open state. RoboClam can vary time scales of motion, forces, and pressures associated with digging to define how to burrow most efficiently [8].

In lab burrowing with RoboClam has helped define the parameter space associated with burrowing. This burrowing is done in a 96 gallon drum filled with 1 mm diameter glass beads. This glass bead media is used since it is a “weaker” soil meaning burrowing can be performed in lab, where an infinite bed of soil is not available. Testing has revealed important parameters associated with burrowing. Contracting too quickly does not give the particles time to move, whereas contracting too slowly lets the particles simply slide along without ever entering a fluidized state. Re-expanding too slowly means the particles have already settled [8].

While RoboClam has elucidated the fundamental behavior of localized fluidization burrowing, it is not close to being a platform for commercial applications. The actuation system is external to the end effector, located above the waterline. The device is also very small; anchoring force from a device this size would be minimal. An advanced design is needed to further understand how a device could be created for anchoring in the ocean. This paper presents the scaling laws that govern the design of devices of all sizes. The next generation RoboClam (RoboClam 2) will be internally actuated and fully waterproof. This device will allow for in lab validation of the scaling laws presented in this paper.

ANALYSIS

Design requirements

Bluefin Robotics, our commercial partner on this project, seeks to use RoboClam technology to anchor their autonomous underwater vehicles to the seafloor. This is a need for several reasons. When anchored, an AUV could stay in one place without using any power, either in ocean currents or in a stream. Sea currents currently cause the AUV to drift, sometimes at up to two knots. This mean the AUV can quickly cover a great deal of undesired distance from a certain location.

There are several important factors to consider when designing an anchoring system for an AUV. The design requirements for RoboClam 2 are as follows.

- A self-contained system with an electrically powered actuator integrated as part of the device and sufficiently powerful for a variety of conditions.
- A device sized to be carried on, and effectively anchor an AUV
- A device that expands radially, improving digging effectiveness.
- Move with proper motion to achieve fluidization with the lowest power possible.

Explanation

RoboClam 2 must be entirely self contained and have internal actuation to allow it to be an anchor for an AUV. This device must be electrically powered since pneumatic or hydraulic systems would be difficult to implement on an AUV, where the energy is stored in batteries.

The overall dimensions of RoboClam 2 must be such that the device will fit inside of an AUV but is large enough that the anchoring force will be sufficient to hold the vehicle in place. RoboClam 2 should be 2-3 inches in diameter to fit within existing ports in the AUV. It should also be short enough to fit inside of the cross section of the AUV - less than 11 inches long for a Bluefin 12 vehicle and 20 inches max for a Bluefin 21 vehicle [3]. These dimensions as well as a physical review of the AUV provided insight for the optimal scale of a device and helped narrow the scope of actuator technologies that work for this application.

Anchoring Force

RoboClam 2 must be large enough to sufficiently anchor an AUV in moving currents. For calculating the size of an anchor and depth at which it needs to be set at, we can compare drag force on a Bluefin AUV with the anchoring force that can be achieved. The drag force on the vehicle is calculated using

$$F_{drag} = \frac{1}{2} C_D \rho_w A_f v_c^2, \quad (1)$$

where C_D is the coefficient of drag, ρ_w is the density of seawater, A_f is the frontal area of the vehicle (with 21” diameter), and v_c is current velocity. For the Bluefin 21 vehicle, $C_D = 0.25$, $\rho_w = 1029 \frac{kg}{m^3}$, $A_f = 0.223 m^2$, and $v_c = 5$ knots [$2.57 \frac{m}{s}$]. This results in a drag force of 203 N for a 5 knot current.

Holding force in the vertical direction for an anchor can be found using

$$F = A(c\bar{N}_c + \Delta\rho g D\bar{N}_q) \left(0.84 + 0.16 \frac{B}{L}\right) \quad (2)$$

which is empirically derived [9], where F is anchoring force, A is the projected area of the anchor normal to the direction of tension, c is the cohesive strength of the soil, \bar{N}_c is a cohesive fitting factor, $\Delta\rho$ is the difference in density between the water and soil, g is the gravitational constant, D is the anchor depth in soil, \bar{N}_q is a buoyancy fitting factor, and $\frac{B}{L}$ is the fluke aspect

ratio. Assuming granular, non-cohesive soils and $(0.84 + 0.16 \frac{B}{L}) \approx 1$ for most fluke shapes yields the following

$$F_{anchor} \approx \bar{N}_q \Delta \rho g A D. \quad (3)$$

Using a least square fit for existing anchoring technologies, we get a buoyancy fitting factor (\bar{N}_q) of 6.2 (which would correspond to a 45° line between the anchor and AUV) [10]. Setting the F_{anchor} equal to the required F_{drag} , a device 2.2 inches in diameter, where $\Delta \rho = 493 \frac{kg}{m^3}$, $g = 9.81 \frac{m}{s^2}$, $A = .002 m^2$ results in a required anchoring depth of 2.75 m for 5 knot currents. A device with greater area (for example by deploying flukes) would not have to go as deep to achieve the same anchoring force.

Fluidized Zone Shape

Achieving uniform fluidization around the entire RoboClam is desirable since this results in the most significant drag reduction. RoboClam 1 is rectangular in cross section and moves in a single degree of freedom when it expands.

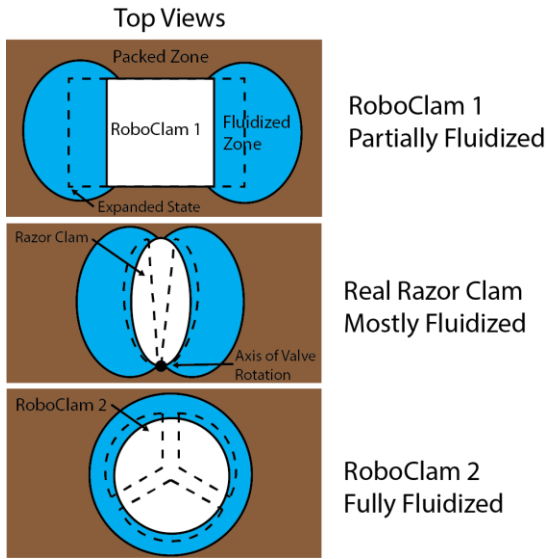


Figure 1: FLUIDIZED ZONE CROSS-SECTION. This figure shows a top view of RoboClam 1, a real razor clam, and the RoboClam 2 design (not to scale). The RoboClam 1 moves in a single direction. Zones to the sides of the direction of motion fluidize, but areas where contraction does not occur do not fluidize. The geometry of razor clams allows them to fluidize a much larger amount of the area around their shell. A hinge on one side of the shell allows it to expand and contract. RoboClam 2 will have full fluidization since it contracts radially. It consists of three shell pieces which move radially outward driven by a wedge.

While this was sufficient for testing, visualization with particle image velocimetry (PIV) revealed that fluidization was only occurring on the sides of the device. Razor clams are oval-shaped and fluidization can occur around almost the entire outer surface, reducing the force needed to burrow. As such, a

radially expanding device was selected as the best solution to get fluidization on the entire outer surface (Fig. 1).

Displacement Required for Sufficient Fluidization

In order to properly size the RoboClam 2 displacement, an analysis of the fluidized volume around the device was performed. This ensures that the shell displacement brings the region around the device to a state beyond incipient fluidization (when the particles just lose contact). In order to know how much the device must contract, it is important to determine how large an area becomes fluidized upon contraction.

Two important soil properties must be measured to determine the radius of the fluidized zone. The first is the coefficient of lateral earth pressure

$$K_0 = \frac{\sigma'_{h0}}{\sigma'_{v0}}, \quad (4)$$

where σ'_{v0} and σ'_{h0} are the vertical and horizontal effective stresses in the soil at undisturbed equilibrium. The second property is the coefficient of active factor

$$K_a = \frac{1 - \sin(\varphi)}{1 + \sin(\varphi)}, \quad (5)$$

where φ is the friction angle of the soil. Using these two parameters, we can calculate the radius of failure R_f [8]

$$\frac{R_f}{R_0} \approx \left(\frac{2}{1 - \frac{K_a}{K_0}} \right)^{\frac{1}{2}}, \quad (6)$$

where R_0 is the expanded radius of the device. R_f predicts the boundary of the fluidized zone. Using a friction angle of 25° for glass beads and the dimensions of the RoboClam 2, $R_f = 2.018$ inches. In this failure radius, we need a change in volume of 6.1 in³ to reach a void fraction of at least 41%. This corresponds to a displacement of the shells of the device of 0.056 inches.

Since this is a very small contraction, we designed RoboClam 2 to have a larger contraction than this (0.25 in) so we can study what happens with very large volume changes. This allows for two types of studies. The first is determining what happens with different amounts of contraction. Since we use an electric actuator, we can control the displacement precisely to determine what the benefits are of different contraction amounts. Second, since the device is capable of much larger contraction than needed, we can also run the device in two configurations, one where it is contracting small amounts from its expanded state, and one where it is contracting small amounts from an almost closed state. This allows for testing of slightly different “diameter” devices which will also be beneficial to determine how accurate the scaling laws are in a laboratory setting.

Minimum Contraction Time

Previous testing of RoboClam 1 suggests a minimum time for contraction, moving faster results in unsuccessful tests. Modeling this time is important to understand how fast a larger device should expand and contract. To determine the velocity, a small control volume (CV) of fluid near the wall of the contracting device is considered (Fig. 2). When contracting, the inside face of the CV has no pressure acting on it, and the outside has hydrostatic pressure. We can relate this pressure to the force for acceleration.

$$F = PA = ma, \quad (7)$$

where P is the pressure acting on the outside surface, A is the area of the outside surface, m is the mass of the fluid volume, and a is its acceleration. For a very small $d\theta$ this shape can be approximated as a right triangle. This simplifies the volume of this shape to $V = \frac{1}{2}L^2d\theta dz$. The area over which hydrostatic pressure (ρgh) is acting is equal to $Ld\theta dz$. Evaluating we get

$$Ld\theta dz\rho gh = \frac{1}{2}L^2d\theta dz\rho a. \quad (8)$$

Cancelling terms and rearranging leaves

$$a = \frac{2gh}{L}. \quad (9)$$

We can approximate $L \approx R_c$ since R_c is a characteristic length of the robot. Integrating twice and cancelling the constants of integration leaves

$$d \approx \frac{gh}{R_c}t^2 \rightarrow t_{\min_fluid} = \sqrt{\frac{dR_c}{gh}}. \quad (10)$$

This means that the time for contraction scales with the square root of RoboClam 2 displacement and its radius, and 1/square root of how deep it is. This means that bigger devices must move slower, taking a longer time to contract, and the deeper the device is, the faster it can move, as would be expected. For a device the size of RoboClam 1 at a depth of 1 m, this yields $t_{\min_fluid} = 0.087$ s.

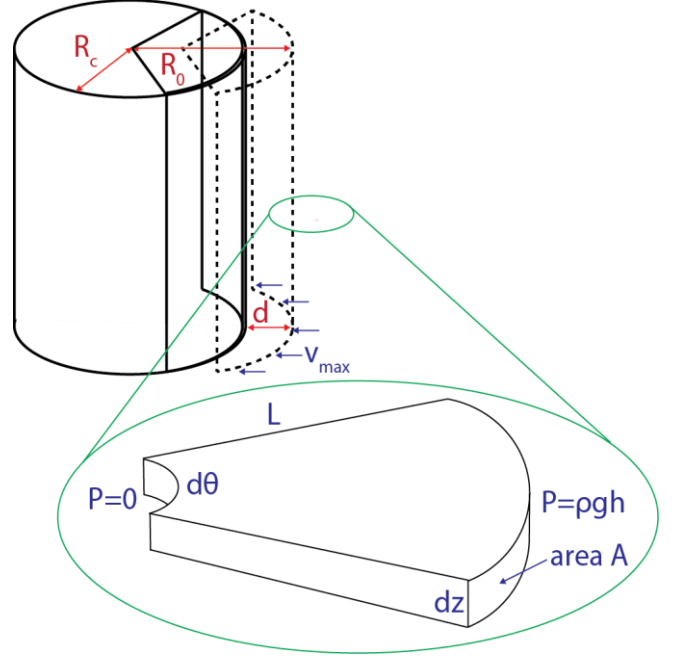


Figure 2: FLUID CONTROL VOLUME. This figure shows a small wedge shaped control volume of fluid at the wall of RoboClam as it is contracting. A force balance can be used on this CV to determine the maximum velocity at which it can be accelerated. This is used to determine the maximum speed at which the RoboClam should move.

A second calculation of the minimum time can be found based on Stokes drag [11]. This is because the fluid Reynolds number of fluid flowing inward as RoboClam contracts is relatively low [12]. The drag on the particles causes them to accelerate and move inward to the fluidized zone. Time is needed for these particles to accelerate, as moving too quickly does not give the particles time to move and the fluidized zone cannot be created. The timescale for a particle to accelerate to the velocity which the shells are moving is

$$m_p \frac{dv_p}{dt} = 6\pi\mu d_p (v_v - v_p) \rightarrow t_{\min_particles} = \frac{d_p^2 \rho_p}{36\mu}, \quad (11)$$

where m_p is the mass of the particle, v_p is the particle velocity, d_p is the diameter of the particle, ρ_p is the density of the particle, v_v is the velocity of a contracting valve, μ is viscosity of the pore fluid, and $t_{\min_particles}$ is the time constant of the differential equation governing velocity change in Stokes flow [11].

Using this formula for RoboClam 1 with 1 mm glass beads in water gives $t_{\min_particles} = 0.075$ s. As can be seen in Fig. 3, the green dots clustered around the times calculated with both this and the previous analysis are successful tests. Moving much faster than this tends to result in tests that are not successful.

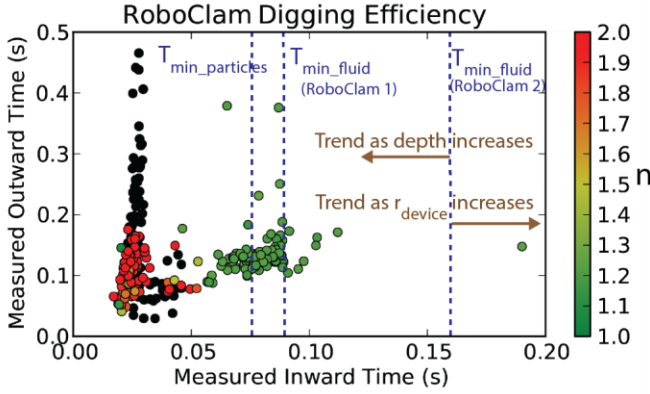


Figure 3: IN LAB BURROWING TESTS. This figure shows lab tests of RoboClam burrowing. The color bar indicates the power law relationship n between energy and depth. Green dots ($n=1$) signify successful tests where fluidization occurred, red ($n=2$) signifies unsuccessful tests with no fluidization, and black is when the robot dug less than one body length deep [12]. The analytical t_{\min} for particles (0.075 s) and the fluid (0.086 s) are labeled on the graph. Successful tests occurred for times approximately equal to the minimum time shown by the cluster of green data points around the minimum times for the fluid and particles, but trials significantly below the minimum time were often unsuccessful (black or red dots). Notice that for larger devices, the t_{\min} for fluid increases (1.68 seconds for a device the size of the RoboClam 2 at 1 meter depth). As the device burrows deeper, the t_{\min} for the fluid decreases meaning that deeper burrowing is likely to require quicker motions.

Downward Drag Force

The design intention for RoboClam 2 is to have it move downward under its own weight through the fluidized zone. While this would not be possible with packed soil, fluidized soil reduces the force required to burrow and can allow an object to move downward. A fluidized soil behaves like a Newtonian fluid with a modified viscosity. The force on a cylinder moving downward through a fluidized burrow can be modeled by [13]

$$F = \pi r^2 \frac{-dp}{dz} L + 2\pi r L \mu_{eff} \frac{d}{dr} [u_c + u_p] \Big|_r, \quad (12)$$

where F is the force, r is the device radius, L is the device length, μ_{eff} is the effective viscosity of the fluid particle mixture, and u_c and u_p are the summed Couette and Poiseuille flows in an annulus of flow upward around the object. Setting this force equal to the underwater weight of the clam (its weight minus the buoyancy force acting on it) will determine the velocity at which RoboClam 2 can travel through the fluidized burrow.

For the RoboClam 2 design, the underwater weight is approximately 40 N of force acting downward. If we set the upward force equal to the mass of the device, we can determine the terminal velocity of the RoboClam in a burrow. Doing this yields $v = 0.489 \frac{m}{s}$ and thus we can expect the device to move downward in the burrow. However, it will likely not have

sufficient time to accelerate to terminal velocity, meaning it will travel at a lower average velocity.

Force for Re-Expansion in Static Soil

Properly sizing the actuator for the RoboClam device was an important part of this design. Since it is easier to move through fluidized soil than packed soil, it was determined that the maximum force that needs to be achieved is when the RoboClam is in a bed of soil in a contracted state, and the particles around the device are settled.

Mohr's circle [14] can be used to represent the stress state in the soil for passive failure (failure resulting from an increase horizontal in stress) for the soil in a settled state [15]. Based on the depth at which the device is embedded, the stress needed to fail the soil can be calculated. The size of the shell then allows the total force needed to be determined.

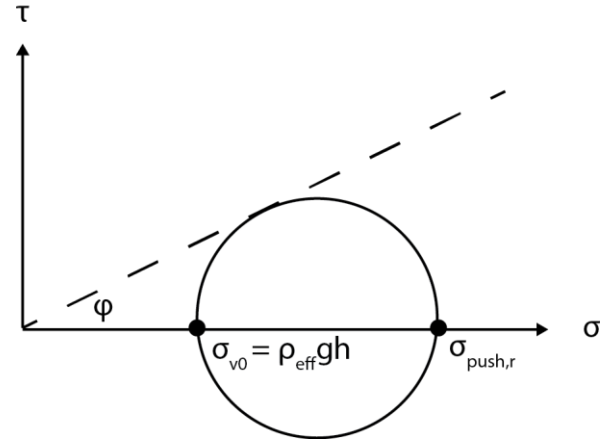


Figure 4: MOHR'S CIRCLE FOR PASSIVE FAILURE. This figure depicts the soil state for passive failure. The depth at which the anchor is set determines how much stress is needed to fail the soil. τ is shear stress, σ is normal stress, ϕ is the friction angle (25 degrees for this media), σ_{v0} is the vertical stress, and $\sigma_{push,r}$ is the horizontal stress.

Solving Mohr's circle at a depth of 1 m where ρ_{eff} is the effective density of the fluid particle mixture at a settled state density ($1980 \frac{kg}{m^3}$, for a fluid, glass bead mixture with a 38% packing fraction) yields a maximum horizontal stress of 47800 Pa (Fig. 4). Multiplying by the projected side area of the RoboClam shell ($.018 m^2$) gives a force of 863 N needed to expand the device in settled soil. The forces needed when the soil is fluidized are less than this number, since it is easier to move through fluidized soil. This value is within the range that the selected actuator is capable of producing for our system

ROBOCLAM 2 DESIGN

Overview

The new RoboClam device consists of an internally located, electric linear actuator, two wedges, one on each end of the device, and three shells which move radially in and out (Fig. 5). Actuation of the linear actuator causes the wedges to

slide against features on the shell resulting in expansion of the device.

A double wedge design was used for actuation of the shells. There are two benefits to this design. Having two wedges prevents the device from jamming since the center of pressure of the soil acts between these two wedges. Locating these features at the ends allows for a smaller diameter, longer device. This is beneficial since power scaling is more favorable for as small diameter of a device as possible.

A 4:1 transmission ratio was selected for the actuation of the RoboClam by controlling the angle of the wedge features that actuate the outer shells. This means that for every 4 linear inches of motion of the linear actuator, the shell sides move outward 1 inch. This ratio was selected for mechanical advantage. The linear actuator is capable of a peak force of 255 N so ignoring friction, this mechanical advantage gives the shells an expansion force of 1020 N. This is beneficial since the actuator is capable of moving very quickly, but has comparably low force to what is needed for a device of this size.

Actuator Selection

An electric actuator was selected for the internally actuated design [16]. Using an electric actuator is desired since it uses the same power source that is readily available in an AUV. It can also have a very high power density and can accelerate much faster than other actuator types. The selected actuator is an excellent choice because it is a radial form factor that can be easily implemented in the RoboClam 2 design. It allows for accurate position control and the ability to control velocity of motion, a benefit over pneumatic actuators. This will allow for probing the characteristic times for digging and lead to discovery of the best timescale, as moving slower requires less power, but moving too slowly will not create the fluidized zone. Friction has been ignored for this model. Sliding components will be lubricated to reduce friction as much as possible. The actuator is also waterproof and corrosion resistant, allowing for testing in water.

CONCLUSION

This paper presents theory for device scaling relationships based on localized fluidization burrowing. These scaling relations are used for designing RoboClam 2. The next step for this project is to create a physical prototype of this device, which will compare test results to theoretical models.

The electric actuator will allow for easy testing of different velocities and displacements in order to validate the scaling laws derived in this paper. RoboClam 2 will allow for further exploration of the contraction and expansion times necessary and how slowly the device can move and still burrow effectively, as this will require lower power. This device will also facilitate testing of the contraction displacements needed to burrow effectively, and the relation between shell displacement and burrowing velocity. The anchoring force achievable with RoboClam 2 will also be explored in comparison with the model presented.

Upon completion of the testing, in-lab performance will be compared with the theory developed in this paper. This will validate the relationships presented and allow for dissemination of design rules to enabling engineers to design different scale devices for a variety of applications.

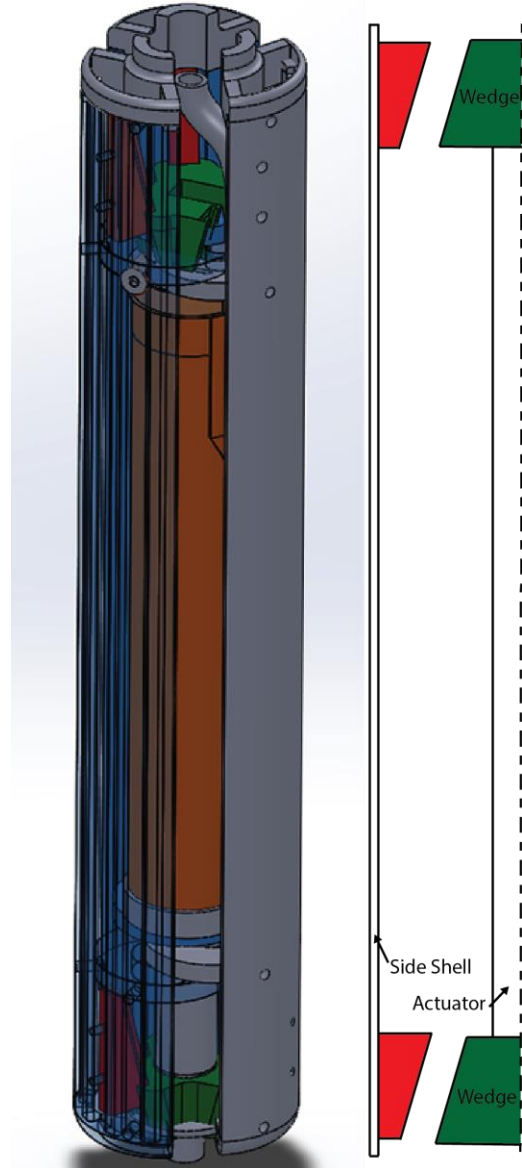


Figure 5: ROBOCLAM 2 DESIGN. Left: This figure shows the model of RoboClam 2. The fluid vents are seen at the very top of the device. Mesh covers these vents and prevents glass beads from entering the device. The power cord for the actuator (orange) is seen bending near the top, so the cord can exit from the middle of the device. Round tabs slide on the end of the actuator and prevent the outer shells from moving along the length of the device. Slots on these round tabs prevent the shells from rotation with respect to the actuator. Seals are attached along the length of the gaps between the three side shells. Right: Side view of the wedge actuation design. The sliding wedge (green) actuates the red tabs on each side shell. This design allows for 4:1 mechanical advantage.

ACKNOWLEDGEMENTS

This work was sponsored by the National Science Foundation Graduate Research Fellowship under Grant No. 1122374 and Bluefin Robotics.

REFERENCES

- [1] Dorgan, K., Jumars, P., Johnson, B., Boudreau, B., and Landis, E., 2005. "Burrowing mechanics: Burrow extension by crack propagation". *Nature*, 433(7025), p. 475.
- [2] Maladen, R., Ding, Y., Li, C., and Goldman, D., 2009. "Undulatory swimming in sand: Subsurface locomotion of the sandfish lizard". *Science*, 325(5938), p. 314.
- [3] Meeting with Bluefin Robotics Jun 3, 2013
- [4] Personal observations by the authors. Jun 2011.
- [5] Holland, A., and Dean, J., 1977. "The biology of the stout razor clam *Tagelus plebeius*: I. Animal-sediment relationships, feeding mechanism, and community biology". *Chesapeake Science*, 18(1), pp. 58–66.
- [6] Winter, V. A., and Hosoi, A., 2011. "Identification and Evaluation of the Atlantic Razor Clam (*Ensis directus*) for biologically inspired subsea burrowing systems". *Integrative and Comparative Biology*, 51(1), pp. 151–157.
- [7] Winter, V. A., Deits, R., Dorsch, D., and Hosoi, A.E., S. A., 2010. "Teaching RoboClam to Dig: The Design, Testing, and Genetic Algorithm Optimization of a Biomimetic Robot". In Proceedings of the IEEE/RSJ 2010 International Conference on Intelligent Robots and Systems (IROS), no. WeET11.3.
- [8] Winter, V. A., Deits, R., Dorsch, D., Slocum, A., and Hosoi, A., 2014. "Razor clam to RoboClam: burrowing drag reduction mechanisms and their robotic adaptation". *Bioinspiration & Biomimetics*.
- [9] M.E. McCormick. 1979. *Anchoring systems*. Pergamon Press, Oxford; New York.
- [10] Winter, A. G., 2011. "Biologically inspired mechanisms for burrowing in undersea substrates." PhD thesis, Massachusetts Institute of Technology, Cambridge, MA.
- [11] Kundu, P., and Cohen, I., 2004. *Fluid Mechanics*. Elsevier Academic Press.
- [12] Winter, V. A., Deits, R., Dorsch, D., 2013. "Critical Timescales for Burrowing in Undersea Substrates Via Localized Fluidization, Demonstrated by Roboclam: A Robot Inspired By Atlantic Razor Clams" In Proceedings of the ASME 2013 International Design Engineering Technical Conferences & Computers and Information in Engineering Conference.
- [13] Winter, V. A., Deits, R., and Hosoi, A., 2012. "Localized Fluidization Burrowing Mechanics of *Ensis directus*". *The Journal of Experimental Biology*, 215(12), pp. 2072–2080.
- [14] Hibbeler, R.C., 2000. *Mechanics of Materials*. Prentice Hall, 4th edition.
- [15] Terzaghi, K., Peck, R., and Mesri, G., 1996. *Soil mechanics in engineering practice*. Wiley-Interscience.

-
- [16] Linmot, 2013. Linear Motor Product Datasheet. http://www.linmot.com/fileadmin/doc/Overviews/Overview_Marketing_e_recent.pdf